COMPARISON OF PRIMARY AND SECONDARY FORMS OF MULTIPLE EVANESCENT WHITE DOT SYNDROME

YASMINE SERRAR, MD,* ARMELLE CAHUZAC, MD,† PIERRE GASCON, MD,‡§¶ CAROLE LANGLOIS-JACQUES, MSc,** MARTINE MAUGET-FAŸSSE, MD,† BENJAMIN WOLFF, MD,†† PASCAL SÈVE, MD, PhD,‡‡ LAURENT KODJIKIAN, MD, PhD,*§§ THIBAUD MATHIS, MD, PhD*§§

Purpose: The aim of this study was to compare primary versus secondary forms of multiple evanescent white dot syndrome (MEWDS) at T0 (baseline) and T1 (1–4 months after the onset of symptoms).

Methods: A total of 101 eyes in 100 patients were included in a multicentric retrospective study.

Results: Secondary MEWDS was defined as MEWDS associated with underlying chorioretinal inflammatory pathologies, mainly multifocal choroiditis and punctuate inner choroidopathy. Patients with secondary MEWDS were older ($P = 0.011$). The proportion of women ($P = 0.8$), spherical equivalent ($P = 0.3$), and best-corrected visual acuity at T0 ($P = 0.2$) were not significantly different between the two groups. The area of MEWDS lesions on late-phase indocyanine green angiography was significantly smaller in secondary MEWDS ($P = 0.001$) and less symmetrical with respect to both horizontal ($P = 0.003$) and vertical ($P = 0.004$) axis. At T0, neither the clinical ($P = 0.5$) nor the multimodal imaging ($P = 0.2$) inflammation scores were significantly different between the groups. At T1, the multimodal imaging inflammation score was higher in secondary MEWDS ($P = 0.021$).

Conclusion: In secondary MEWDS, outer retinal lesions are less extensive and located close to preexisting chorioretinal lesions. Mild signs of intraocular inflammation on multimodal imaging are more frequent in secondary MEWDS during recovery. These findings suggest that chorioretinal inflammation may trigger secondary MEWDS.

RETINA 42:2368–2378, 2022

Multiple evanescent white dot syndrome (MEWDS) is defined as a transient retinal inflammatory disease characterized by discrete white dots disseminated on the fundus and associated with foveal granularity.[1] It is most often unilateral, but bilateral forms do exist.[2] The classic form of MEWDS usually affects young, slightly myopic, female patients and resolves spontaneously within a few weeks. Some authors have hypothesized that MEWDS may be triggered by a viral infection as many patients describe flu-like symptoms preceding the vision loss, but there is no formal evidence of this to date.[1] Fundus autofluorescence (FAF) provides key information with hyperautofluorescent spots and dots, which disappear after retinal photobleaching.[3] Fluorescein angiography (FA) is poorly specific and shows "wreath-like" hyperfluorescence, whereas late-phase indocyanine green angiography (ICGA) shows multiple hypofluorescent spots and dots, colocalizing with, but outnumbering the hyperautofluorescent lesions.[4] Spectral domain optical coherence tomography (SD-OCT) shows areas of disruption of the ellipsoid zone (EZ) corresponding to large hyperautofluorescent and hypofluorescent lesions on ICGA: these lesions are called "spots."[5–7] The second type of lesions found on SD-OCT is hyperreflective spicules in the outer nuclear layer (ONL) that colocalize with punctate hyperautofluorescent and hypofluorescent lesions on ICGA: these lesions are called "dots."[6,7] Moreover, in the very early stages of the disease, SD-OCT shows a subfoveal hyperreflective dome-shaped lesion.[8] These multimodal imaging findings for MEWDS suggest that the disease may be caused by inflammation of photoreceptors.[6,7] Other authors argue that photoreceptor dysfunction in MEWDS could be secondary to retinal pigment epithelium (RPE) damage.[9–11]

Since the first description by Jampol,[1] several cases of MEWDS "overlapping" with other retinal diseases have been reported. Numerous authors have described MEWDS occurring at the same time as multifocal choroiditis (MFC) or punctuate inner choroidopathy (PIC),[12–14] some questioning whether MEWDS and MFC/PIC share the same pathogenesis.[13,15] Furthermore, it has been reported that choroidal neovascularization (CNV), including CNV secondary to choriocapillaritis (such as MFC and PIC), may trigger MEWDS.[16] MEWDS-like lesions have also been reported in ocular toxoplasmosis (OT),[10] pseudoxanthoma elasticum,[17] Best disease—with or without CNV[12,18]—and even after retinal detachment surgery.[19] Recently, Essilfie et al[19] described forms of secondary MEWDS which they have termed "Epi-MEWDS" and suggest that it could be caused by damage to the RPE or Bruch membrane. In short, MEWDS could either be idiopathic or triggered by a preexisting or underlying chorioretinal disease. Throughout this article, we will refer to the idiopathic forms of MEWDS as "primary MEWDS." When MEWDS is associated with an underlying chorioretinal disease, it will be referred to as "secondary MEWDS."

In this study, we aim to compare the multimodal imaging characteristics of primary and secondary forms of MEWDS, to define their clinical spectrum.

METHODS

Patient Selection

We retrospectively reviewed the records of patients diagnosed with MEWDS between July 2010 and August 2021 in several retinal reference centers across France (Hospices Civils de Lyon–Lyon; Fondation Rothschild– Paris; Centre Monticelli–Marseille). The diagnosis, based on the multimodal imaging characteristics of MEWDS described above, was confirmed by at least two retinal specialists (Y.S., A.C., B.W., or P.G.). Any disagreements were assessed by a third senior examiner (L.K., M.M.F., or T.M.). Patients who did not meet the diagnosis criteria or had insufficient multimodal imaging at baseline or during follow-up were excluded. This research was conducted in accordance with the Declaration of Helsinki. An international review board approved this study (Ethics Committee of the French Society of Ophthalmology, IRB 00008855 Société Française d'Ophtalmologie IRB#1).

Data Collection

We collected patient demographics, medical history, clinical, and multimodal imaging features at baseline and during the follow-up. Examinations included best-corrected visual acuity (BCVA), slit-lamp examination, dilated fundus examination, and multimodal imaging. Fundus photographs were obtained using either Eidon retinograph (CenterVue, Padova, Italy) or the ultra-wide-field Optos California system (Optos PLC, Dunfermline, Scotland, United Kingdom). SD-OCT, FAF, FA, and ICGA were performed using SPECTRALIS SD-OCT and HRA (HRA SPECTRALIS, Heidelberg Engineering, Heidelberg, Germany).

Findings were recorded at baseline during the acute phase (T0) up to 4 weeks after the onset of symptoms. T1 lasted from 1 month up until 4 months after the onset of symptoms,[6] and T2 from 4 months after the onset of symptoms until the end of follow-up. If the patient attended multiple appointments during T1, we selected the one with most complete multimodal imaging.

Bilateral MEWDS was defined as the presence of multimodal imaging features consistent with MEWDS in both eyes at the same time. In these cases, both eyes were included. Complete medical records were screened for the whole follow-up period. A recurrence was defined as a new episode of MEWDS occurring in the same or the contralateral eye, after complete recovery from the first episode, evidenced on multimodal imaging.

Group of Patients

The patients were divided into two groups (primary or secondary MEWDS) by the panel of retinal specialists. MEWDS was defined as secondary if any underlying ocular pathology had been diagnosed before T0, at T0, or during T1 or T2. Paraclinical tests such as laboratory testing or CT scans/MRIs were not prescribed systematically, but at the ophthalmologists' discretion.

Outcome Measures

Patient demographics and disease characteristics were compared between the two groups. The image characteristics were also analyzed.

From the *Service d'Ophtalmologie, Hôpital universitaire de la Croix-Rousse, Hospices Civils de Lyon, Lyon, France; †Fondation Ophtalmologique Adolphe de Rothschild, Paris, France; ‡Department of Ophthalmology, Aix-Marseille University, Hopital Nord, Marseille, France; §Centre Monticelli Paradis, Marseille, France; ¶Groupe Almaviva Santé, Clinique Juge, Marseille, France; **Service de Biostatistiques, Hospices Civils de Lyon, Lyon, France; ††Centre Ophtalmologique Maison Rouge, Strasbourg, France; ‡‡Service de Médecine Interne, Hôpital universitaire de la Croix-Rousse, Hospices Civils de Lyon, Lyon, France; and §§Laboratoire UMR-CNRS 5510 Matéis, Villeurbanne, France.

None of the authors has any financial/conflicting interests to disclose.

Reprint requests: Thibaud Mathis, MD, PhD, Service d'Ophtalmologie, Hôpital Universitaire de la Croix-Rousse–Hospices Civils de Lyon, 103, Grande Rue de la Croix-Rousse, 69317 Lyon cedex 04, France; e-mail: thibaud.mathis@chu-lyon.fr

Area of Multiple Evanescent White Dot Syndrome Lesions on Late-Phase Indocyanine Green Angiography

The area of MEWDS lesions on late-phase ICGA was measured for each eye at T0 on the 55° images centered on the macula obtained with SPECTRALIS HRA (Heidelberg Engineering). Late-phase ICGA images were captured between 20 and 35 minutes after the intravenous injection. All images were adjusted to the same size (1536 × 1536 pixels) and resolution (87.5 pixels per inch). The freehand tool in the ImageJ software program (version 2.1.0/1.53c, https://imagej.net) was used to manually draw the borders of the hypofluorescent lesions on late-phase ICGA. Before any measurements were taken, the software was calibrated according to the scale bar (200 μm) for all the FAF and ICGA images captured using SPECTRALIS HRA (Heidelberg Engineering). Fundus autofluorescence images were used to distinguish MEWDS lesions from other hypofluorescent structures or lesions on ICGA. Because MEWDS lesions are hyperautofluorescent, the borders of the hypoautofluorescent areas on the optic disc and retinal lesions causing secondary MEWDS were drawn using the freehand tool on the FAF images and then subtracted from the total area of hypofluorescence on late-phase ICGA. The selected areas were saved in the Region of Interest (ROI) manager to calculate the area of MEWDS lesions in mm^2. Measurements were not taken when the borders of the hypofluorescence were not visible because of poor quality ICGA images.

We divided the area of MEWDS lesions by the total area of the ICGA image (250 mm^2 for each image after calibrating size and resolution as explained above) to obtain the percentage of pathological area on the ICGA image. The horizontal symmetry of MEWDS lesions was assessed based on a horizontal axis passing through the center of optic disc and the fovea: we compared the area of MEWDS lesions located above and below the axis with a "horizontal symmetry ratio" of 0 to 1. The vertical symmetry of MEWDS lesions was assessed based on a vertical axis passing through the center of optic disc. We defined a peripapillary area within a circle with a radius of 3.6 mm (twice the standard disc diameter of 1.8 mm)[20] centered on the optic disc. Within this peripapillary area, we compared the area of MEWDS lesions located on the nasal and temporal sides of the vertical axis with a "vertical symmetry ratio" of 0 to 1. For both ratios, the numerator was the smallest hypofluorescent area (whether it was superior, inferior, temporal, or nasal) and the denominator was the largest area. A ratio of 0 meant no lesions were found on one side of the axis, and a ratio of one meant equal areas of MEWDS lesions were measured on both sides of the axis (Figure 1).

Fundus Autofluorescence

Fundus autofluorescence images were recorded at T0 and T1. Owing to the poorer quality of FAF images compared with ICGA images, we decided not to measure the area of hyperautofluorescent lesions on the FAF images because the measurements would have been less accurate. However, for each case, we determined whether hyperautofluorescent and hypofluorescent lesions on ICGA colocalized and whether similar symmetry ratios were observed on the FAF and ICGA images.

Subfoveal Choroidal Thickness

Subfoveal choroidal thickness (CT) was measured at T0 and T1 on SD-OCT scans with or without enhanced depth imaging (EDI), whenever the posterior limit of choroid was seen, using the caliper function (Heidelberg Eye Explorer V.5.6.1.0; Heidelberg Engineering, Heidelberg, Germany). Eighteen patients treated with steroids before the onset of symptoms or during follow-up were excluded from the CT analysis.

Inflammation Scores

A clinical inflammation score of 0 to three was defined at T0 and T1 as follows: one point for anterior chamber inflammation, one point for vitritis, and one point for optic disc edema.

A multimodal inflammation score was defined at T0 and T1 as follows: one point for papillitis on FA (defined as papillary leakage on FA), one point for vasculitis on FA (defined as retinal vascular leakage on FA), and one point for vitritis on SD-OCT (defined as the presence of hyperreflective dots in the vitreous on SD-OCT).

Statistics

Categorical variables are presented as numbers and percentages, whereas continuous variables are presented as mean and SD or medians and interquartile range [IQR]. For categorical variables, the comparisons between the groups were calculated using the Chi-square test. For continuous variables, the comparisons between the groups were calculated using the *t*-test or the nonparametric Mann–Whitney test according to the normality. A P-value < 0.05 was considered statistically significant. All analyses were performed using SAS version 9.4 (SAS Institute Inc, Cary, NC).

RESULTS

A total of 101 eyes in 100 patients were included in our study: 60 eyes with primary MEWDS in 59 patients and 41 eyes with secondary MEWDS. Secondary

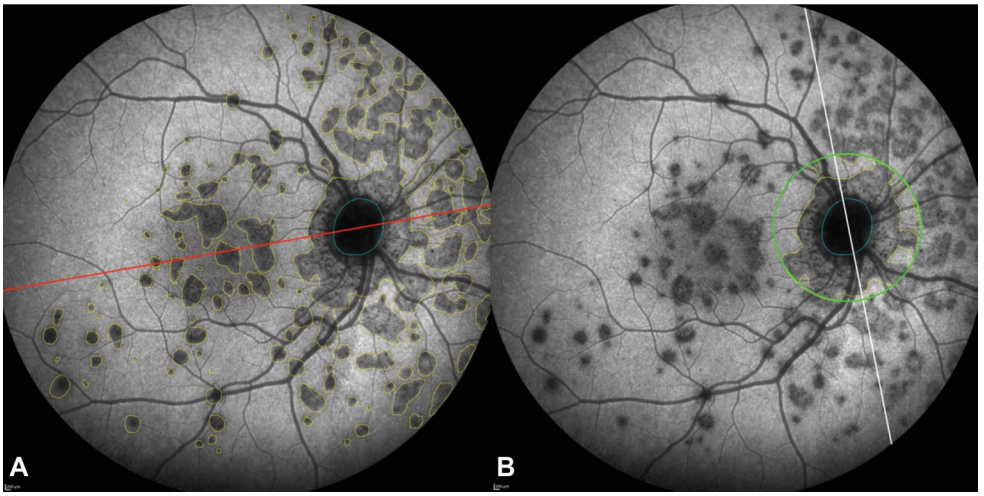

Fig. 1. Methodology used to measure MEWDS lesions on late-phase ICGA. **A.** Hypofluorescence on late-phase ICGA was bordered in ImageJ using the freehand tool (yellow borders). The surface area of MEWDS lesions on the posterior pole was measured after subtracting the hypoautofluorescence from the optic disc or chorioretinal lesions (blue borders). To assess the symmetry of MEWDS with respect to a horizontal axis (red line), we compared the area of MEWDS lesions above and below a horizontal axis with a ratio from 0 to 1. **B.** We defined a peripapillary area (green circle) within a circle with a radius of 3.6 mm centered on the optic disc. To assess the symmetry of MEWDS with respect to a vertical axis (white line), we compared the area of MEWDS lesions within the green circle on the nasal and temporal side of a vertical axis with a ratio from 0 to 1.

MEWDS included patients with PIC/MFC who was active, inactive, or complicated by CNV; other inflammatory diseases of the posterior segment; CNV with various etiologies; and unspecific atrophic scars (Table 1, Figure 2 and 3). One patient (1.0%) had bilateral primary MEWDS. The median [IQR] period between the onset of symptoms and the first appointment (T0) was not significantly different between the two groups, at 9.5 days [5.0–14.0] for primary MEWDS and 7.0 days [6.0–12.0] days for secondary MEWDS.

In secondary MEWDS, the underlying pathology had been diagnosed before T0 in 20 patients (48.8%) within a median [IQR] period of 24.0 [1.5–66.0] months, at T0 in 18 patients (43.9%), and at T1 or T2 in three patients (7.3%) within a median [IQR] period of 2.0 months [1.8–3.5]. When the underlying pathology was chronic and could recur (i.e., all etiologies except atrophic scars), MEWDS occurred at the same time as disease recurrence in 30 patients (76.9%).

After the onset of symptoms, the median [IQR] duration of follow-up was 2.0 [0.3–9.8] months for primary MEWDS and 19.0 [3.0–36.0] months for secondary MEWDS. At T0, FAF was performed on 97 eyes (96.0%), SD-OCT on 95 eyes (94.1%), FA on 86 eyes (85.1%), and ICGA on 84 eyes (83.2%). The area of MEWDS lesions on ICGA was not measured in six patients with secondary MEWDS, although the ICGA images were available. In one case, the ICGA image had been captured too late (60 minutes), resulting in the absence of visible hypofluorescence. The other five patients all had MEWDS lesions around chorioretinal scars because of MFC/PIC, and the ICGA hypofluorescence of MEWDS could not be precisely distinguished from choroiditis. At T1, ophthalmologic findings were collected for 83 eyes (82.2%). FAF was obtained for 63 eyes (62.4%), SD-OCT for 73 eyes (72.3%), FA for 19 eyes (18.8%), and ICGA for 20 eyes (19.8%).

Patient Characteristics and Clinical Characteristics at T0

The mean (SD) age of the whole cohort was 28.4 (11.0) years, and patients were mostly women (n = 81, 82.0%).

Table 1. Etiologies of MEWDS

Etiologies	N (Eyes)
Primary MEWDS	**60**
Secondary MEWDS	**41**
PIC/MFC	**24**
Active PIC/MFC	10
Inactive PIC/MFC	5
Complicated by CNV	9
Other inflammatory diseases of posterior segment	**9**
Ocular toxoplasmosis	7
Birdshot chorioretinopathy	1
Optic neuritis on multiple sclerosis	1
CNV (etiology other than PIC/MFC)	**6**
Best disease	2
Atrophic scar on congenital ocular toxoplasmosis	1
Idiopathic atrophic scar	1
Coloboma of optic papilla (Figure 2)	1
Idiopathic CNV	1
Atrophic scars (etiology other than PIC/MFC and without CNV)	**2**
Cryotherapy on peripheral retina	1
Radiotherapy to treat retinoblastoma (Figure 3)	1

MEWDS, multiple evanescent white dot syndrome; MFC, multifocal choroiditis; PIC, punctuate inner choroidopathy; CNV, choroidal neovascularization.

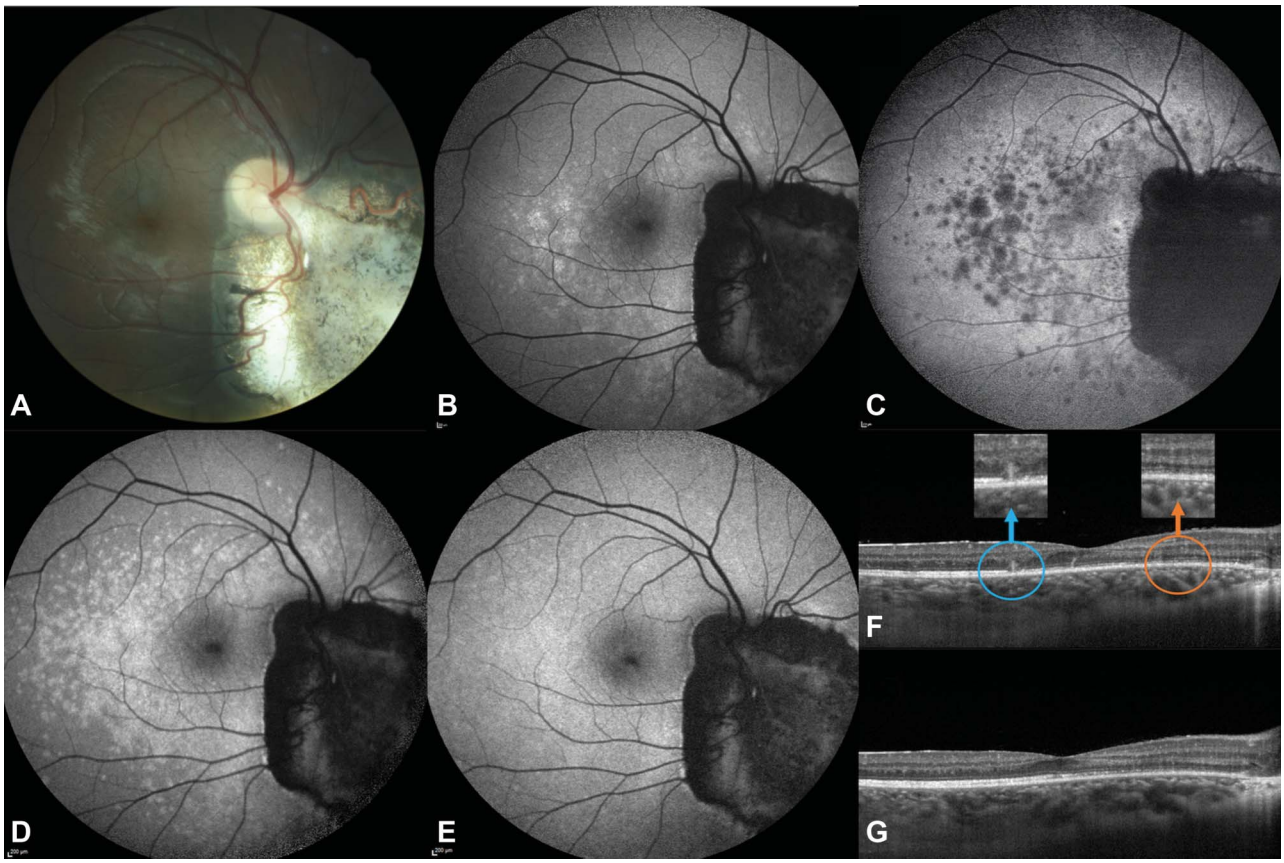

Fig. 2. Secondary MEWDS in a 22-year-old woman with a history of retinoblastoma treated with radiotherapy in the right eye. **A.** Retinography 8 days after the onset of symptoms showing the retinal scar from the retinoblastoma with no sign of recurrence. The visual acuity was measured at 20/40 in this eye. **B.** FAF 8 days after the onset of symptoms showing hyperautofluorescent spots and dots. **C.** Late phase of ICGA demonstrating corresponding hypofluorescent lesions. **D.** FAF 15 days after onset showing an increase in MEWDS lesions. **E.** FAF 2 months after onset showing partial retinal recovery. **F.** SD-OCT 8 days after onset, showing spicules (blue circle), and EZ disruptions (orange circle). **G.** SD-OCT 2 months after onset demonstrating a decrease in the spicules, but some areas of EZ disruption were still visible.

The mean (SD) spherical equivalent was −2.0 (3.5) diopters. Patients with secondary MEWDS were older (P = 0.011), with fewer visible spots or dots on the fundus (P = 0.013) at T0. The proportion of women (P = 0.8), spherical equivalent (P = 0.3), BCVA (P = 0.2), and presence of previous flu-like symptoms (P = 0.1) was not significantly different between the groups. No difference was found in the clinical (P = 0.5) and multimodal imaging (P = 0.2) inflammation scores in primary versus secondary MEWDS. Finally, CT was not significantly different between the groups (P = 0.1) (Table 2).

Comparison of the Spatial Distribution of Multiple Evanescent White Dot Syndrome Lesions

The area of MEWDS lesions on late-phase ICGA was significantly smaller in secondary MEWDS (P = 0.001). The mean (SD) pathological area represented 40.6% (23.2) of the total surface area of the ICGA image in primary MEWDS compared with 19.0% (12.5) in secondary MEWDS. Within the peripapillary area defined above, the area of MEWDS lesions was also significantly smaller in secondary MEWDS (P = 0.018).

The distribution of MEWDS lesions was less symmetrical with respect to both horizontal (P = 0.003) and vertical (P = 0.004) axis in secondary MEWDS (Table 3).

When the chorioretinal lesion supposedly causing the MEWDS was located either on the superior or inferior hemiretina (n = 16), the MEWDS lesions were larger in the hemiretina containing the chorioretinal lesion in 16 eyes (100%). When the chorioretinal lesion supposedly causing the MEWDS was located either on the nasal or temporal hemiretina (n = 22), MEWDS lesions in the peripapillary area were larger in the hemiretina containing the chorioretinal lesion in 81.8 eyes (81.8%) (Figure 4).

Concerning the spatial distribution of MEWDS lesions on FAF images, the visual comparison of FAF and ICGA images showed hyperautofluorescent and hypofluorescent lesions on ICGA colocalized. Similar symmetry ratios were observed on FAF images compared with ICGA images but were not measured, as explained above.

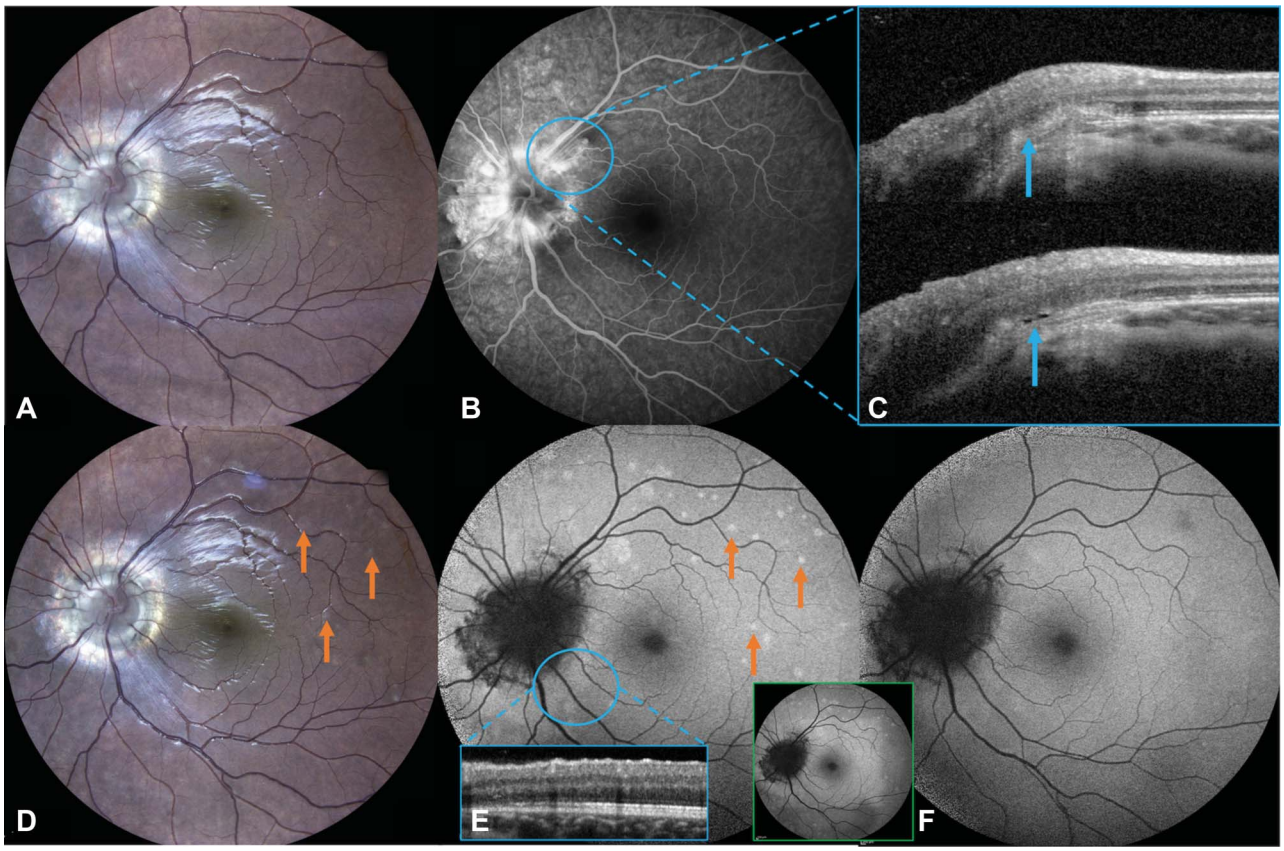

Fig. 3. Secondary MEWDS in a 19-year-old woman with a history of optic nerve coloboma complicated by choroidal neovascularization. **A.** Retinography before the occurrence of MEWDS showing the optic coloboma. The patient complained of blurred vision in her left eye (visual acuity: 20/32). **B.** Fluorescein angiography showing superior peripapillary leakage. **C.** SD-OCT demonstrating a peripapillary pigmented epithelial detachment associated with subretinal hyperreflective material and subretinal fluid (blue arrows). Choroidal neovascularization was suspected, although it was difficult to confirm the diagnosis on FA because of the optic nerve coloboma. The patient was treated with an intravitreal injection of ranibizumab. **D.** Retinography 1 month later, showing discrete white dots on the fundus. The patient was still complaining of blurred vision (visual acuity: 20/32). **E.** Fundus autofluorescence demonstrating hyperautofluorescent lesions (orange arrows), associated with ellipsoid zone disruptions on SD-OCT (blue square). The hyperautofluorescent lesions disappeared after retinal photobleaching (green square). **F.** FAF was normalized 1 month later.

Evolution of Multiple Evanescent White Dot Syndrome

The median [IQR] time from the onset of symptoms to T1 was not significantly different between groups with 63.5 days [47.0–90.3] for primary and 64.0 days [52.8–93.3] for secondary MEWDS ($P = 0.7$). At T1, the mean BCVA was better for primary MEWDS ($P = 0.006$). Moreover, the multimodal imaging inflammation score was lower in primary MEWDS compared with secondary MEWDS ($P = 0.021$). None of the other clinical nor imaging characteristics were found to be significantly different between the two forms of MEWDS. The difference in CT between T0 and T1 was not significantly different between the two groups ($P = 0.6$, Table 4).

Overall, a total of 18 patients experienced MEWDS recurrence (18.0%). MEWDS recurrences were not significantly more frequent in primary MEWDS (8 patients, 13.6%) compared with secondary MEWDS (10 patients, 24.4%, $P = 0.2$). The median [IQR] time to recurrence was not statistically different in primary MEWDS (12.0 [5.8–17.3] months) as opposed to secondary MEWDS (34.0 [14.8–49.0] months). Recurrences in the contralateral eye occurred in two patients (3.4%) with primary MEWDS and two patients (4.9%) with secondary MEWDS. Recurrences of secondary MEWDS were always associated with a recurrence of the underlying pathology in the same eye (n = 10 patients, 100%).

Discussion

The main finding of our study is that the hypofluorescent lesions on late-phase ICGA were less extensive and less symmetric in secondary MEWDS than in primary MEWDS. Moreover, we observed that the MEWDS lesions were mostly located in the same quadrant as the chorioretinal lesions supposedly causing the MEWDS. One hypothesis regarding the

Table 2. Patient Characteristics and Clinical Examinations at Baseline (T0)

	Primary MEWDS	Secondary MEWDS	*P*
Sex, female, n (%)	48 (82.8)	33 (80.5)	0.8
Mean age, years (SD)	26.1 (9.3)	31.7 (12.3)	**0.011**
Mean spherical equivalent, diopters (SD)	−1.4 (2.6)	−2.7 (4.2)	0.3
Median time from onset to T0, days [IQR]	9.5 [5.0–14.0]	7.0 [6.0–12.0]	0.6
Mean BCVA, logMAR (SD)	0.2 (0.2)	0.3 (0.3)	0.2
Flu-like symptoms, n (%)	11 (20.0%)	3 (7.9%)	0.1
Visible spots or dots on the fundus, n (%)	45 (86.5%)	23 (63.9%)	**0.013**
Clinical inflammatory signs, n (%)			
0 point	36 (73.5%)	26 (72.2%)	0.5
1 point	11 (22.4%)	6 (16.7%)	
2 points	2 (4.1%)	3 (8.3%)	
3 points	0	1 (2.8%)	
Multimodal imaging inflammatory signs, n (%)			
0 point	5 (8.5%)	2 (4.9%)	0.2
1 point	16 (27.1%)	17 (41.5%)	
2 points	25 (42.4%)	10 (24.4%)	
3 points	13 (22.0%)	12 (29.3%)	
Mean choroidal thickness, μm (SD)	347.6 (78.3)	310.0 (87.6)	0.1

pathogenesis of secondary MEWDS is that damage to subretinal tissue may alter the posterior retinal–blood barrier and trigger transient major inflammation in the outer retina.[17,19] Therefore, inflammation of the outer retina may start around the initial chorioretinal lesions and spread secondarily, explaining why secondary MEWDS is less extensive. In cases of MEWDS secondary to optic neuritis, the inflammation may spread through contiguity from the optic nerve to the retina, resulting in MEWDS.

Our results support the hypothesis that secondary MEWDS may be caused by locally triggered inflammation of the outer retina. This implies that a MEWDS trigger should be suspected in MEWDS cases where FAF or ICGA show few lesions or lesions not centered on the posterior pole. These results suggest that all patients with MEWDS should undergo a complete ophthalmologic examination including FAF which is a fast and noninvasive way of assessing the size and symmetry of MEWDS lesions. FA and ICGA should also be included in follow-up for patients with MEWDS because they are essential when searching for a MEWDS trigger.

The main underlying pathologies supposedly causing secondary MEWDS were MFC and PIC. This association has been well-described in the literature.[12–14] Other etiologies found herein have also been previously reported in association with MEWDS in "overlap" syndromes: CNV,[16] Best disease,[12,18] OT,[10] and optic neuritis.[21] To the best of our knowledge, MEWDS secondary to Birdshot chorioretinopathy has never been reported. No other cases of MEWDS secondary to atrophic scars after radiotherapy or cryotherapy have been described in the literature, but Essilfie et al[19] reported MEWDS in a patient with a history of vitreoretinal surgery for retinal detachment. The demographics of patients with primary and secondary MEWDS were similar. In both groups, patients were mostly young and myopic women. Patients with secondary MEWDS were significantly older, but the mean age was still young. This is not surprising because patients with MEWDS and MFC/PIC share the same demographics.[15] Therefore, MEWDS in a young myopic female patient should not be considered as primary without further investigation. There was no significant difference between primary and secondary MEWDS at baseline regarding signs of ocular inflammation. Mild clinical and paraclinical signs of intraocular inflammation are classic features of primary MEWDS[1,22] and are also found in most of the inflammatory etiologies overlapping secondary MEWDS. Therefore, the presence of inflammatory signs at baseline cannot help distinguish between primary and secondary MEWDS.

CT was not significantly thicker or thinner in secondary MEWDS at T0 and decreased in both primary and secondary MEWDS at T1. Although it

Table 3. Spatial Distribution of MEWDS Lesions at Baseline (T0)

	Primary MEWDS	Secondary MEWDS	*P*
Mean area of MEWDS lesions on late-phase ICGA on the posterior pole, mm^2 (SD)	99.5 (59.1)	47.5 (31.1)	**0.001**
Mean area of MEWDS lesions within the peripapillary area, mm^2 (SD)	11.3 (6.3)	7.4 (6.5)	**0.018**
Mean horizontal symmetry ratio (0–1), (SD)	0.8 (0.2)	0.7 (0.3)	**0.003**
Mean vertical symmetry ratio (0–1), (SD)	0.8 (0.3)	0.6 (0.4)	**0.004**

Bold entries are for statistically significant *p*-values (< 0.05).

has been previously been shown that CT increases during the acute stage of PIC and decreases after resolution,[23] the findings for MEWDS are less clear. Some authors have reported a significant decrease in CT after MEWDS recovery in the eye with MEWDS[24] or in both eyes even in unilateral MEWDS.[25] Yet other studies have found this decrease in CT to be neither statistically significant nor clinically relevant.[6,7] Kang et al[14] showed that eyes with MEWDS secondary to MFC had thicker choroids compared with eyes with primary MEWDS in the acute phase, suggesting a thicker choroid could be a sign of more severe inflammation. Our results found comparable CT at T0 and a comparable decrease in CT at T1 suggesting that measuring CT is probably not useful when attempting to distinguish between a secondary and primary form of

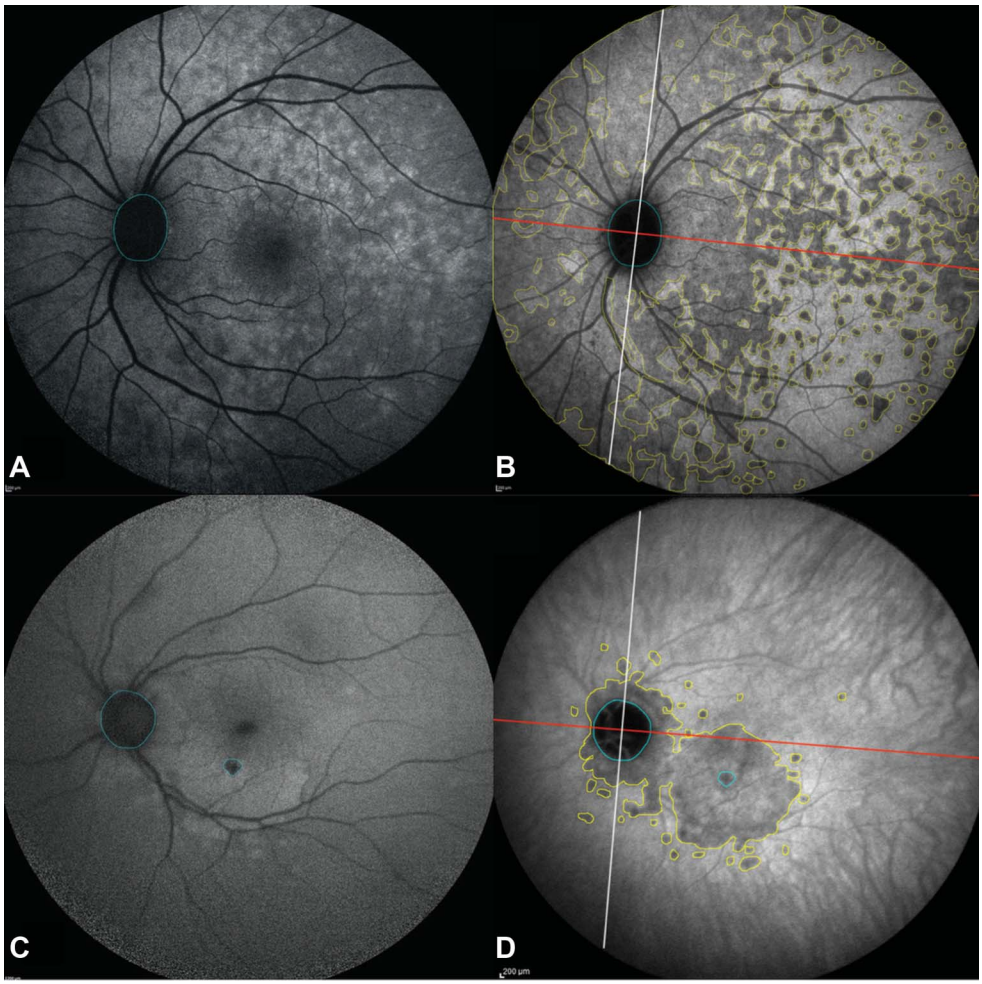

Fig. 4. Cases of ICGA hypofluorescence measurements in a primary form and secondary form of MEWDS. **A and B.** FAF shows hyperautofluorescent lesions in a case of primary MEWDS. The area of MEWDS lesions on ICGA is 150.8 mm^2 (60.3% of the surface area of ICGA image), and the horizontal symmetry ratio is 0.9. **C and D.** FAF shows a hypoautofluorescent chorioretinal lesion consistent with PIC (confirmed by multimodal imaging), surrounded by hyperautofluorescent secondary MEWDS lesions. Hypoautofluorescent areas from optic disc and PIC (blue borders) were subtracted from hypofluorescence on ICGA (yellow borders) to keep the MEWDS lesions only. The area of MEWDS lesions is 41.7 mm^2 (16.7% of the surface area of ICGA image), and the horizontal symmetry ratio is 0.2.

Table 4. Evolution of Primary and Secondary MEWDS at T1 and During Follow-Up

	Primary MEWDS	Secondary MEWDS	*P*
Median time from onset to T1, days [IQR] (N = 83)	63.5 [47.0–90.3]	64.0 [52.8–93.3]	0.7
Mean BCVA at T1, logMAR (SD) (N = 83)	0.0 (0.1)	0.2 (0.3)	**0.006**
Fundus spot and dots at T1, n (%) (N = 83)	6 (18.2%)	4 (11.8%)	0.5
Clinical inflammatory signs at T1, n (%) (N = 69)			
0 point	35 (100.0%)	32 (94.1%)	0.3
1 point	0	1 (2.9%)	
2 points	0	1 (2.9%)	
3 points	0	0	
Multimodal imaging inflammatory signs at T1, n (%) (N = 75)			
0 point	28 (73.7%)	15 (40.5%)	**0.021**
1 point	8 (21.1%)	15 (40.5%)	
2 points	2 (5.3%)	4 (10.8%)	
3 points	0	3 (8.1%)	
Persistent hyperautofluorescent lesions at T1, n (%) (N = 63)	12 (37.5%)	11 (35.5%)	0.9
Persistent ICGA hypofluorescent lesions at T1, n (%) (N = 20)	3 (30.0%)	4 (40.0%)	0.6
Persistent irregularity of EZ or hyperreflective dots in ONL on SD-OCT at T1, n (%) (N = 73)	27 (75.0%)	28 (75.7%)	0.9
Mean choroidal thickness change between T0 and T1, μm (SD) (N = 73)	−20.1 (23.7)	−23.8 (21.4)	0.6

Bold entries are for statistically significant *p*-values (< 0.05).

MEWDS. However, the comparison of CT in our study has several limitations. First, the patients with secondary MEWDS were significantly older, and the mean spherical equivalent was lower in secondary MEWDS. Because age and axial length are inversely correlated with CT, our study may have failed to prove a difference in CT between the two groups because of these confounding factors.[26] Second, CT measurements can be imprecise due to fluctuations.[27]

The evolution of primary and secondary MEWDS at T1 was similar except for BCVA which was significantly worse in secondary MEWDS: some patients still had low BCVA because of foveal damage caused by the underlying pathology.[14] Moreover, some subclinical inflammation may have been present at T1, as reported on the multimodal imaging that showed significantly more frequent inflammatory signs in secondary MEWDS.

There was only one case of simultaneous bilateral primary MEWDS in the present cohort. In the literature, cases of simultaneous bilateral MEWDS are rarely reported even in the largest primary[28,29] or secondary[18,19] MEWDS cohorts. It is not clear whether these apparently rare cases of simultaneous bilateral forms of MEWDS are more frequently primary or secondary. Concerning recurrence, it was expected to be more frequent in secondary MEWDS because the underlying pathology itself is likely to recur, but no statistically significant difference was found in our study. This is not so surprising because cohorts of primary MEWDS actually report recurrence rates of 11% to 14%.[28,29] It is important to note that recurrences of secondary MEWDS in the contralateral eye were always associated with a recurrence of the underlying pathology in the same eye. When the underlying condition was unilateral, MEWDS recurrences remained unilateral, which corroborates the hypothesis regarding the pathogenesis of secondary MEWDS suggested above.

Our study has several limitations. The first of which is the short follow-up period, especially for primary MEWDS. Once recovery is complete, the follow-up in a referral center is not always recommended. Moreover, patients with primary MEWDS often failed to attend their follow-up appointments. However, follow-up was longer for primary patients with MEWDS who made a slow recovery or experienced recurrences and for patients with secondary MEWDS because the underlying pathology required frequent check-ups. To overcome this

potential bias, we decided to compare final clinical and multimodal imaging findings at T1, from 1 to 4 months after the onset of symptoms, rather than comparing data from each patient's last visit. A second limitation is that MEWDS management was not standardized across all the centers. At T0, FA and ICGA were missing for a few eyes. At T1, multimodal imaging was incomplete for most patients and angiography was rarely repeated. Therefore, some secondary MEWDS with a silent underlying pathology may have been misclassified as primary MEWDS because of missing data. However, the multimodal imaging and medical investigations made it possible to newly diagnose an underlying pathology in 21 patients during follow-up. Furthermore, certain differential diagnoses could not be formally excluded because additional imaging and laboratory testing were not mandatory for MEWDS. However, given the follow-up of patients with MEWDS and the inclusion of patients from retinal and uveitis reference centers only, the risk of misdiagnosis was limited. A multicentric prospective study with a standardized patient management at diagnosis and during follow-up including systematic ophthalmological and paraclinical examinations could be interesting but would be difficult to set up given the low incidence of MEWDS. Another limitation is in the definition of T0 and T1. Here, we considered the acute phase (T0) up until 4 weeks after the first symptoms, as previously defined,[6] and T1 between 1 and 4 months. This could be considered to be a very wide range for each period because MEWDS lesions can regress rapidly, but the median times from the onset of symptoms to T0 and T1 were more or less comparable between primary and secondary MEWDS. Furthermore, a narrower definition of the acute phase would have excluded many patients who consulted the reference centers a few weeks after their first symptoms, when the MEWDS lesions were still clearly visible. Finally, the measurement of MEWDS lesions could not be computerized due to the uneven brightness on the ICGA images. Manual measurements were therefore more accurate. All the measurements were taken by the same investigator (YS) to limit measurement bias. However, the measurements could not be taken for six patients with secondary MEWDS because of poor quality images. The evaluation of the vertical and horizontal symmetry of MEWDS lesions could be more precise using ultra-wide-field (UWF) imaging rather than a 55° ICGA image centered on the macula, especially for the vertical symmetry ratio. Unfortunately, UWF imaging systems were not commonly used when we began this study (July 2010), and even today, not all the participating centers are equipped with these devices.

In conclusion, this study analyzed a large cohort of patients with primary and secondary MEWDS. Both forms of MEWDS typically concern young myopic women. Lesions of the outer retina in secondary MEWDS are less extensive and localized near the chorioretinal lesions supposedly causing the MEWDS. This finding suggests that local chorioretinal damage because of a proinflammatory underlying pathology may trigger MEWDS. Conversely, a MEWDS trigger should be suspected in cases of MEWDS with asymmetrical lesions on the posterior pole or few hyperautofluorescent lesions on FAF. An underlying pathology should also be suspected in cases with persistent signs of inflammation on multimodal imaging. Recurrent and bilateral forms were not more frequent in secondary MEWDS, but further studies are needed to confirm these results.

Key words: inflammation, multiple evanescent white dot syndrome, retinochoroiditis.

References

1. Jampol LM, Sieving PA, Pugh D, et al. Multiple evanescent white dot syndrome. I. Clinical findings. Arch Ophthalmol 1984;102:671–674.
2. Meyer RJ, Jampol LM. Recurrences and bilaterality in the multiple evanescent white-dot syndrome. Am J Ophthalmol 1986;101:388–389.
3. Freund KB, Mrejen S, Jung J, et al. Increased fundus autofluorescence related to outer retinal disruption. JAMA Ophthalmol 2013;131:1645–1649.
4. Gross NE. Multiple evanescent white dot syndrome. Arch Ophthalmol 2006;124:493.
5. Spaide RF, Koizumi H, Freund KB. Photoreceptor outer segment abnormalities as a cause of blind spot enlargement in acute zonal occult outer retinopathy-complex diseases. Am J Ophthalmol 2008;146:111–120.
6. Pichi F, Srvivastava SK, Chexal S, et al. En face optical coherence tomography and optical coherence tomography angiography of multiple evanescent white dot syndrome: new insights into pathogenesis. Retina 2016;36:S178–S188.
7. Marsiglia M, Gallego-Pinazo R, Cunha de Souza E, et al. Expanded clinical spectrum of multiple evanescent white dot syndrome with multimodal imaging. Retina 2016;36:64–74.
8. Cahuzac A, Wolff B, Mathis T, et al. Multimodal imaging findings in "hyper-early" stage MEWDS. Br J Ophthalmol 2017;101:1381–1385.
9. Gaudric A, Mrejen S. Why the dots are black only in the late phase of the indocyanine green angiography in multiple evanescent white dot syndrome. Retin Cases Brief Rep 2017;11:S81–S85.
10. Mathis T, Delaunay B, Favard C, et al. Hyperautofluorescent spots in acute ocular toxoplasmosis: a new indicator of outer retinal inflammation. Retina 2020;40:2396–2402.
11. Zicarelli F, Mantovani A, Preziosa C, Staurenghi G. Multimodal imaging of multiple evanescent white dot syndrome: a new interpretation. Ocul Immunol Inflamm 2020;28:814–820.
12. Bryan RG, Freund KB, Yannuzzi LA, et al. Multiple evanescent white dot syndrome in patients with multifocal choroiditis. Retina Phila PA 2002;22:317–322.
13. Kuznetcova T, Jeannin B, Herbort CP. A case of overlapping choriocapillaritis syndromes: multimodal imaging appraisal. J Ophthalmic Vis Res 2012;7:67–75.

14. Kang HG, Kim TY, Kim M, et al. Expanding the clinical spectrum of multiple evanescent white dot syndrome with overlapping multifocal choroiditis. Ocul Immunol Inflamm 2022;30:81–89.
15. Jampol LM, Wiredu A, Mfc PIC, Amn AIBSE; AZOOR. One disease or many? Retina 1995;15:373–378.
16. Mathis T, Delaunay B, Cahuzac A, et al. Choroidal neovascularisation triggered multiple evanescent white dot syndrome (MEWDS) in predisposed eyes. Br J Ophthalmol 2017;102:971–976.
17. Gliem M, Birtel J, Müller PL, et al. Acute retinopathy in pseudoxanthoma elasticum. JAMA Ophthalmol 2019;137:1165.
18. Cicinelli MV, Hassan OM, Gill MK, et al. A multiple evanescent white dot syndrome–like reaction to concurrent retinal insults. Ophthalmol Retina 2020;5:1017–1026.
19. Essilfie J, Bacci T, Abdelhakim AH, et al. Are there two forms of multiple evanescent white dot syndrome?. Retina 2022;42: 227–235.
20. Kodjikian L, Rezkallah A, Decullier E, et al. Early predictive factors of visual loss at 1 Year in neovascular age-related macular degeneration under anti–vascular endothelial growth factor. Ophthalmol Retina 2022;6:109–115.
21. Conrady CD, Sassalos T, Cornblath WT, et al. Temporally independent association of multiple evanescent white dot syndrome and optic neuritis. Graefes Arch Clin Exp Ophthalmol 2021;259:2807–2811.
22. Standardization of Uveitis Nomenclature (SUN) Working Group, Jabs DA, Brezin AP, et al. Classification criteria for multiple evanescent white dot syndrome. Am J Ophthalmol 2021;228:198–204.
23. Hirooka K, Saito W, Hashimoto Y, et al. Increased macular choroidal blood flow velocity and decreased choroidal thickness with regression of punctate inner choroidopathy. BMC Ophthalmol 2014;14:73.
24. Pellegrini M, Veronese C, Bernabei F, et al. Choroidal vascular changes in multiple evanescent white dot syndrome. Ocul Immunol Inflamm 2021;29:340–345.
25. Aoyagi R, Hayashi T, Masai A, et al. Subfoveal choroidal thickness in multiple evanescent white dot syndrome. Clin Exp Optom 2012;95:212–217.
26. Michalewski J, Michalewska Z, Nawrocka Z, et al. Correlation of choroidal thickness and volume measurements with axial length and age using swept source optical coherence tomography and optical low-coherence reflectometry. Biomed Res Int 2014;2014:639160.
27. Chakraborty R, Read SA, Collins MJ. Diurnal variations in axial length, choroidal thickness, intraocular pressure, and ocular biometrics. Invest Ophthalmol Vis Sci 2011;52:5121.
28. Bosello F, Westcott M, Casalino G, et al. Multiple evanescent white dot syndrome: clinical course and factors influencing visual acuity recovery. Br J Ophthalmol 2022;106: 121–127.
29. Ramakrishnan MS, Patel AP, Melles R, Vora RA. Multiple evanescent white dot syndrome: findings from a large northern California cohort. Ophthalmol Retina 2021;5:850–854.